Evaluation of Fault Analysis Tool under Power Swing and Out-of-Step Conditions

Ahad Esmaeilian, *Student Member, IEEE* and Mladen Kezunovic, *Fellow, IEEE*
Department of Electrical and Computer Engineering, Texas A&M University
College Station, Texas, 77843, USA
Emails: ahadesmaeilian@tamu.edu, kezunov@ece.tamu.edu,

***Abstract*— Several major blackouts were caused by distance relay mis-operation. Distance relay mis-operation may occur following a large disturbance in the system causing power swing and out-of-step conditions. If an on-line fault analysis tool is able to detect power swing or out-of-step conditions and indicate mis-operation of relays, the operator may be notified to switch back the healthy transmission lines tripped due to relay mis-operation. A new automated fault analysis tool comprising fault detection, classification and location has been developed and its performance under various power swing and out-of-step conditions is reported. The test results indicate that the fault analysis tool performs better than distance relay under power swing and out of-step conditions and can be used as a tool to verify distance relay operation in practical circumstances. The simulations have been performed using IEEE118 bus test system modeled in ATP software.**

***Index Terms*--Fault diagnosis, power swing, out-of-step, power system faults, synchronized sampling.**

I. Introduction

NOWADAYS, power system deregulation resulting in operation close to its limits result in growing number of cascading outages. Power swings are proven to have drawbacks on distance relay operation [1, 2]. As reported in [3], during August 14, 2003 blackout, several distance relays mis-operated in third zone under power swing conditions. As a result, verifying quickly and accurately whether the transmission line (TL) which has been tripped by distance relays indeed has experienced a fault will be beneficial.

Conventional schemes to detect and classify faults proposed earlier are based on voltages, currents and impedances measurements. Identifying fault types using positive and zero sequence impedances of the TL is proposed in [4, 5]. In [6], authors proposed an overcurrent based method which compares superimposed fault currents to identify faulty phases. It needs threshold values to operate correctly which may decrease robustness of the proposed method. Applying Fourier analysis in [7], authors proposed a method to classify fault by measuring magnetic field in one point.

In the recent decades, several researchers focused their study to detect and classify faults on Artificial Neural Network (ANN) based methods [8-14]. In [8, 9], a neural network based high speed fault detection and classification method which could be utilized either as a real time or off line tool was proposed. A self-organized neural network method to detect and classify fault types which applies Adaptive Resonance Theory (ART) with Fuzzy K-nearest neighbor (K-NN) decision rule has been presented in [10]. In [11, 12], a decision-tree based algorithm for detection and classification of fault in both single and double circuit TL has been introduced. In general, ANN based methods need large amount of training samples to cover wide range of operating conditions (varying system loading, fault resistance, fault inception instance, etc.) to be successful in detecting and classifying the faults.

A setting-free method based on two-end synchronized reactive power measurement is presented in [15]. The reactive power flow direction at two ends of the line is used to detect and classify the fault types. While the method is setting-less, calculating the phasor values and average values of power in each cycle could be a source of delay in operation of the algorithm and can be considered as a major drawback for a real time fault detection and classification tool.

Generally, irrespective of how high the accuracy of fault analysis tools in detecting and classifying a fault, these methods should be able to detect power swing or out-of-step conditions. As a result, the operator can switch back the healthy transmission lines whenever relays mis-operate due to power swing or out-of-step conditions. As a result, study of the distance relay algorithm performance as well as fault analysis methods under power swing and out-of-step condition has an important impact on improving power system reliability.

In this paper, we focus on evaluating the performance of simple fault analysis tool developed in previous works by the authors under different power swing and out-of-step conditions [16, 17]. This fault analysis tool compares the change of direction of instantaneous powers computed at two ends of a TL utilizing synchronized voltage and current samples measured at both ends. The tool is very fast and can detect, classify and locate fault without need for phasor computation.

The test results illustrate that the fault analysis tool is hardly affected by this conditions and could be applicable as a relay operation confirmation tool to correct the relay mis-operations.

The work reported in this paper is funded by ARPA-E to develop RATC solution under GENI contract 0473-1510.

A. Esmaeilian and M. Kezunovic are with the Department of Electrical and Computer Engineering, Texas A&M University, College Station, TX 77843-3128, USA (emails: ahadesmaeilian@neo.tamu.edu, kezunov@ece.tamu.edu).

II. Overview of Power Swing and Relay Mis-operation

This section contains discussion of the power swing and out of step (OST) phenomena and their influence on distance relay protection with graphical and mathematical representations.

A. Power Swing Phenomena

In steady state condition of power system, the generated and consumed power maintain equivalent. When system experience a large disturbances, the electrical power at generator bus changes while the mechanical power input to the generators remains constant causing the oscillations in machine rotor angles and result in power swings [18]. If the swing is stable, the fluctuations die down. However, unstable swings result in progressive separation of angle between two areas of the power system, causing large swings of power, large fluctuations of voltages and currents and eventual loss of synchronism between such areas known as out of step (OOS) condition.

Discrimination between faults (especially 3-phase fault) and power swings may become difficult when these large fluctuations of voltage and current occur during power swing. Conventional impedance calculations methods suggest similar conditions as under system faults. Therefore, the impedance trajectory may enter the impedance zone of distance relays [19].

B. Relay Mis-operation

Both stable and unstable power swings will cause problems for distance protection. For stable swings, relay must be blocked to prevent incorrect trips, while in the case of unstable ones, relay must operate to separate unsynchronized areas and prevent further outages [20]. A controlled trip at an electrical center can be desirable during unstable swings. In such condition, the control center may command to several relays to divide the power system into separate stable subsystems. The out-of-step detection logic at the electrical center distinguishes between stable power swings where the system recovers and an unstable out-of-step condition where the grid needs to be separated. The detailed study on impacts of both stable and unstable power swing on distance relay operation are given in [18-20]. According to Fig.1, when there is no fault on the transmission line, the impedance seen by distance relay installed on bus1 is:

$$Z_{meas} = \frac{V_1}{I_1} = \frac{V_1}{\frac{(V_1 - V_2)}{Z_L}} = Z_L \left(\frac{1}{1 - \left|\frac{V_2}{V_1}\right| \angle \theta_{21}} \right) \quad (1)$$

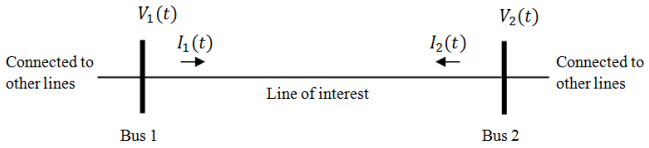

Fig. 1. Transmission line with two-end measurements.

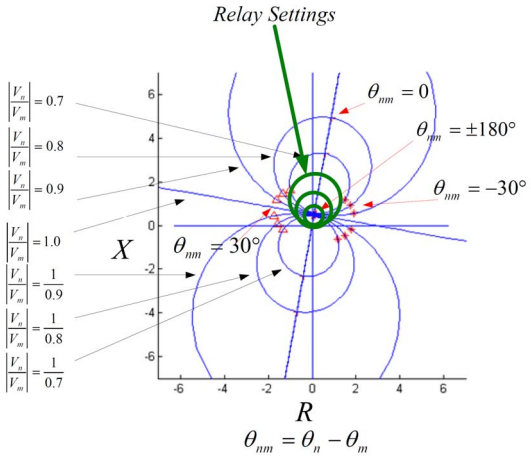

Fig.2. Z_c trajectory in the R-X phase

Fig. 2. Measured impedance trajectory in the R-X plane.

In (1), the measured impedance (Z_{meas}) seen by relay depends on the magnitude ratio and the angle difference of the voltages at the two ends. During power swings, due to oscillation of the bus voltages and line currents, the measured impedance seen by the relay may enters the zone settings results in relay mis-operation. The plots of measured impedance trajectories in the R-X plane with respect to voltage magnitude ratios and angle differences is shown in Fig. 2, under the condition of $Z_L = 1\angle 80^\circ$ [21].

To detect swings and prevent unwanted trips, conventional distance relays equipped with power swing blocking (PSB) module. The PSB module operates based on the rate-of-change of the locus of the apparent impedance during system instability. For a stable swing, this rate-of-change is slow whereas for an instable swing, it is quick. As illustrated in Fig. 2, by defining outer zones or blinders, depending on the type of relay characteristic which is installed, one can measure the time interval required by the apparent impedance locus to cross the two characteristics (buffer area), if the time exceeds a specified value, then the power swing blocking function is initiated.

III. Proposed Fault Analysis Tool

A. Fault Deteciont and Classification

A simple method which compares the change of direction of instantaneous power computed at two ends of a transmission line using time-stamped voltage and current samples measured at both ends is originally proposed in [17]. In Figure 1, $V_1(t)$ and $I_1(t)$ represents voltage and current measured at one end (Bus 1) of the line at instance t. Similarly $V_2(t)$ and $I_2(t)$ represents voltage and current measured at other end (Bus 2) of the line at instance t. Currents are measured in the direction shown in Figure 1. Instantaneous powers calculated at both ends are:

$$P_1(t) = V_1(t) \times I_1(t) \quad (1)$$

$$P_2(t) = V_2(t) \times I_2(t) \quad (2)$$

Now we will discuss a unique feature of this instantaneous power under different types of fault which helps detect and classify faults without using any threshold. During the normal operation, $P_1(t)$ and $P_2(t)$ will be in phase opposition to each other for the current directions assumed. However, for the faulty phases, right after fault inception, they will be almost in-phase with each other. For un-faulted phases the phase opposition will be maintained even after the fault inception. For change in load level the phase relationship does not get reversed but changes according to the load angle difference. So this method can discriminate load level changes from faults.

To represent this feature mathematically, we use signum function which is defined as:

$$\operatorname{sgn}(x) = \begin{cases} -1, & x < 0 \\ 0, & x = 0 \\ 1, & x > 0 \end{cases} \tag{3}$$

We calculate $\operatorname{sgn}(P_1(t))$ and $\operatorname{sgn}(P_2(t))$ and plotted the difference for each phase.

$$P\operatorname{sgn}(t) = \operatorname{sgn}(P_1(t)) - \operatorname{sgn}(P_2(t)) \text{ for phase a,b,c} \tag{4}$$

Theoretically, before a fault this difference $P\operatorname{sgn}(t)$ should be ± 2 and after fault $P\operatorname{sgn}(t)$ should be 0 on all faulty phases, but due to transients and noise present in the measurements, some outliers are present. We used this change of difference of sgn() to detect fault instant. We have used a moving window of 5ms to check whether at least 80% of $P\operatorname{sgn}(t)$ are zero, which indicates a fault. More details on fault detection and classification algorithm through waveforms and results can be found in [17].

B. Fault Location

The synchronized sampling-based fault location scheme proposed in [17] is used here with several improvements. As described in detail in [17], simplified form of fault location equation for short transmission line can be obtained as:

$$d_S = \frac{-\sum_{m=a,b,c}\sum_{k=1}^{N} P_m(k)Q_m(k)}{\sum_{m=a,b,c}\sum_{k=1}^{N} Q_m^2(k)} \tag{5}$$

where:

$$P_m(k) = v_{mR}(k) - v_{mS}(k) - d\sum_{p=a,b,c}\begin{bmatrix} \left(R_{mp} + \left(L_{mp}/\Delta t\right)\right) i_{pR}(k) \\ -\left(L_{mp}/\Delta t\right) i_{pR}(k-1) \end{bmatrix}$$

$$Q_m(k) = d\sum_{p=a,b,c}\begin{bmatrix} \left(R_{mp} + \left(L_{mp}/\Delta t\right)\right)\left[i_{pR}(k) + i_{pS}(k)\right] \\ -\left(L_{mp}/\Delta t\right)\left[i_{pR}(k-1) + i_{pS}(k-1)\right] \end{bmatrix} \tag{6}$$

$m = a,b,c$

k is the present sample point; Δt is the time period with respect to the sampling frequency; subscripts S and R stand for the values at sending end and receiving end respectively. For long transmission line, following recursive equations are derived:

$$v_j(k) = \begin{bmatrix} (1/2)\left[v_{j-1}(k-1) + v_{j-1}(k+1)\right] \\ +\left(Z_c/2\right)\left[i_{j-1}(k-1) - i_{j-1}(k+1)\right] \\ +\left(R\Delta x/4\right)\left[i_{j-1}(k+1) - i_{j-1}(k-1)\right] \end{bmatrix} \tag{7}$$

$$i_j(k) = \begin{bmatrix} \left(1/2Z_c\right)\left[v_{j-1}(k-1) - v_{j-1}(k+1)\right] \\ +(1/2)\left[i_{j-1}(k-1) + i_{j-1}(k+1)\right] - \left(R\Delta x/2Z_c\right) i_j(k) \\ -\left(R\Delta x/4Z_c\right)\left[i_{j-1}(k-1) + i_{j-1}(k+1)\right] \end{bmatrix} \tag{8}$$

where $\Delta x = \Delta t / \sqrt{LC}$ is the distance that the wave travels with a sampling time step Δt, $Z_C = \sqrt{L/C}$ is the surge impedance, subscript j is the position of the discretized point of the line, and k is the sample point. Since the explicit form of fault location cannot be obtained from (7) and (8), following steps are applied to calculate the location of fault:

1. Building of voltage profile utilizing both ends voltage measurements and discretizing the line into equal segments with length of Δx and considering each segment as a short line model.
2. Finding the point that has the minimum square of voltage difference calculated from both ends which represent the approximate fault location.
3. Build a short line model surrounding the approximate fault point, and refine fault location using (5).

The proposed method is highly accurate and reliable while the sampling rate needs to be high (20 kHz or more). To improve the fault location algorithm we used the interpolation method to estimate the voltage and current samples when the sampling frequency in not high enough to mitigate the algorithm requirement. By adding this feature to the proposed method the algorithm is able to calculate the fault location with the lower sampling rate as well (1 kHz) with the same precision as before.

The Flowchart of the fault analysis tool is shown in Fig. 3 which is a summary this section. As it can be seen, the method is initiated after a relay trips a line. Synchronized voltage and current measurements from both ends of the line are gathered and fault detection and classification for all the phases for the single line or both of the parallel lines are calculated. After the fault is detected and classified, the fault location algorithm is performed [17].

IV. Evaluation of Fault Analysis Tool Against Power Swing and Out-of-Step

In this paper, we use Alternative Transient Program (ATP) to model the IEEE118 bus test system to perform realistic simulations.

Fig. 3. Flowchart of the proposed fault detection and classification scheme

A. IEEE118 bus test system on ATP

To be close to the real situations, the power swing needs to be simulated in a dynamic system. The generator dynamic parameters should be known for the simulated system. In ATP model, "SM59" synchronous machine module is used for generator modeling. Power swing is generated by the disturbances such as line fault, load changing and line switching at locations elsewhere of the system. More details about modeling of the IEEE118 bus test system in ATP can be found in the previous works [22].

B. Case1: Different Fault resistance,Type and Location

The proposed method is tested for several simulated fault cases on lines 8–30 of the IEEE 118-bus test system. The line length is 82 miles. The sampling frequency for voltage and current measurements is 1 kHz. The distance to fault from one end of a line is changed to 5%, 20%, and 50% of the line length with fault resistance changes 0, 20, and 100. Table I provides the summary of the results for different types of faults under varying fault distance and resistance. The proposed method detects and classifies fault using a 5ms data window after fault inception on the post-fault data. In all cases, the algorithm detects the faults in less than 6ms, identifies the correct fault types and the fault location accuracy is within 3% except for one case.

Since in this paper the focus is to evaluate the tool against the power swing and out-of-step condition, no more results have been reported on the variation fault cases; however, one can find more results on fault conditions in Ref. [17].

TABLE I
SUMMARY OF FAULT ANALYSIS UNDER VARYING FAULT DISTANCES AND FAULT RESISTANCES

Fault Type	Fault Distance (%)	Fault Resistance (Ω)	Detected Fault Type	Time to detect (ms)	Fault Location % Error
ag	5	0	ag	4.8	1.71
	20		ag	5.2	0.43
	50		ag	5	0.09
	5	20	ag	4.9	1.23
	20		ag	5.1	0.43
	50		ag	5	0.09
	5	100	ag	5.3	0.52
	20		ag	5.3	0.41
	50		ag	5	0.09
ab	5	0	ab	3	2.26
	20		ab	2.6	0.08
	50		ab	2.5	0.19
abg	5	0	abg	3.9	2.26
	20		abg	3.9	0.08
	50		abg	3.9	0.19
	5	20	abg	3.9	1.08
	20		abg	3.9	0.24
	50		abg	3.9	0.18
	5	100	abg	3.9	1.48
	20		abg	3.9	0.05
	50		abg	3.9	0.23
abc	5	0	abc	4.7	1.16
	20		abc	3.9	2.71
	50		abc	5	0.64
	5	20	abc	5.2	0.13
	20		abc	5.1	2.94
	50		abc	4.9	0.004
	5	100	abc	5.5	2.92
	20		abc	5.5	3.17
	50		abc	5.5	0.14

C. *Case2: Stable Power Swing*

To study the effect of power swing, several disturbances including line fault, load changing and line switching at locations elsewhere of the buses that voltages and currents are measured have been simulated. Fig. 4 shows the phase A current measured at bus 26, while a 3phase fault occurred in line (8-30) at 0.25sec and cleared at 0.3sec by tripping that line. As it can be seen, the current waveform swings after tripping of the line (8-30) which in this case is called stable swing.

Figs. 5(a-c) depict the instantaneous power measured from both ends while Figs. 5(d-f) indicate the output sgn value of the fault detection algorithm. However, in several samples, the output value is zero, most of the samples are ± 2. As it already mentioned, since the output value is not equal to zero for more than 80% in any consecutive 5ms time window, no fault will be detected by fault analysis tool. In this case and all other cases which have been simulated no fault is detected which verify the robustness of the tool to distinguish between fault and stable power swing.

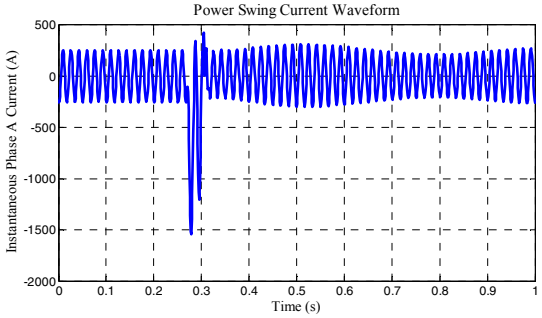

Fig. 4. Current waveform during stable power swing

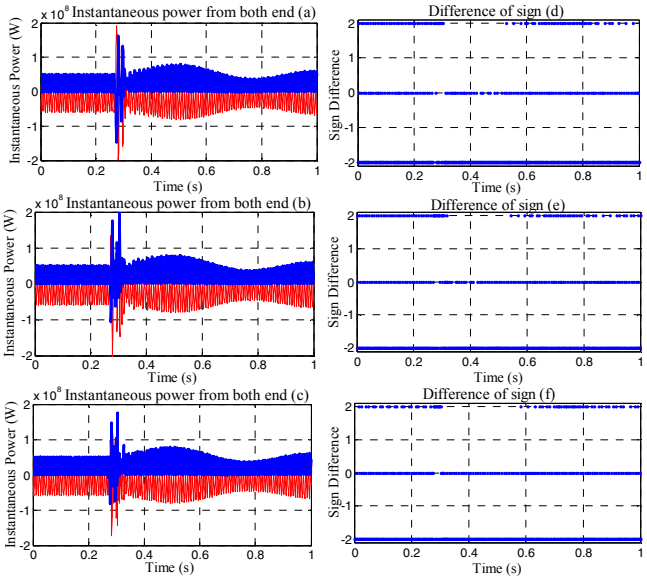

Fig. 5. (a-c): $P\mathrm{sgn}(t)$ with respect to time during stable power swing; (d-f): $P\mathrm{sgn}(t)$ with respect to time during stable power swing.

D. *Case3: Out of Step Condition*

The same procedure is followed to simulate unstable power swing condition which results in out-of-step. The only difference was selecting lines with higher flow of power or longer fault duration to put more stress on the overall system. Fig. 6 shows the phase A current measured at bus 44, while a 3phase fault occurred in line (30-38) at 0.1sec and cleared at 0.28sec by tripping that line. As it can be seen, the current waveform swings after tripping of the line (30-38). As can be seen, at time 0.58sec, the power swing become unstable and two end buses angles start slipping in opposite directions causing out-of-step occur.

Figs. 7(a-c) depict the instantaneous power measured from both ends while Figs. 7(d-f) indicate the output sgn value of the fault detection algorithm. However, in several samples, the output value is zero, most of the samples are ± 2. As it already mentioned, since the output value is not equal to zero for more

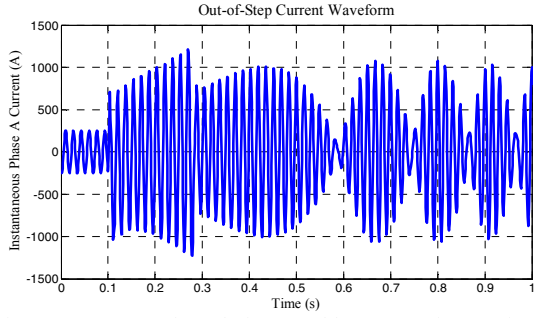

Fig. 6. Current waveform during unstable power swing causing out-of-step

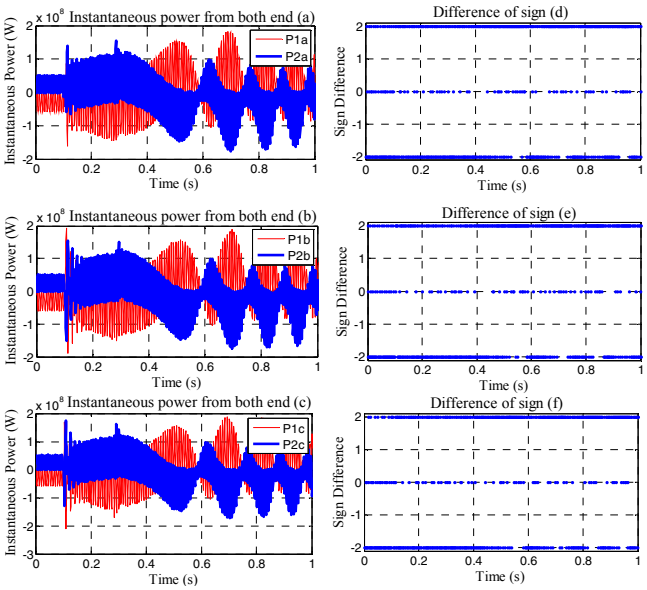

Fig. 7. (a-c): *P*sgn(*t*) with respect to time during stable power swing; (d-f): *P*sgn(*t*) with respect to time during stable power swing.

than 80% in any consecutive 5ms time window, no fault will be detected by fault analysis tool. In this case and all other cases which have been simulated no fault is detected which verify the robustness of the tool to distinguish between fault and stable power swing. It should be noticed that in the case of out-of-step condition, however, the tool is able to distinguish between fault and out-of-step condition, it cannot verify that the power swing is stable or unstable.

V. CONCLUSION

This paper analyzes the issue of power swing and Out-of-Step conditions and is focusing on evaluating synchronized sampling based fault detection, classification and location algorithm [17] during power swing. Based on the theoretical analysis and ATP simulations, the following conclusions can be drawn:

- The fault analysis tool accurately and swiftly detect, classify and locate faults inside the transmission line if the synchronized samples from both line ends are used.
- For power swing issue, it is a concern that it may cause distance relay to trip an un-faulted line. That is unacceptable for a stressed system and may cause cascading blackouts. While in the case of unstable swings causing out-of-step, the relay should trip before the system become unstable and blackout occurs.
- The fault analysis tool is dependable and secure under power condition. It can distinguish faults from power swing and out-of-step conditions; however, it cannot differentiate between stable and unstable conditions. So, it cannot be used as a substitute for out-of-step relays.
- Since in most cases of relays mis-operation, the relay fails to block the trip signal during power swing, the fault analysis tool can be utilized to monitor the operation of distance relay and modify the decision of relay in real-time.

REFERENCES

[1] D. Tziouvaras and D' Hou, "Out-of-Step Protection Fundamentals and Advancements," *30th Annual Western Protective Relay Conference*, October 21-23, 2003, Spokane, Washington.

[2] M. Jonsson, "Line Protection and Power System Collapse," Master's Thesis, Department of Electric Power Engineering, Chalmers University of Technology, Goteborg, Sweden, 2001.

[3] "Final Report on the August 14, 2003 Blackout in the United States and Canada: Causes and Recommendations," U.S.-Canada Power System Outage Task Force, April 5, 2004.

[4] M. S. Sachdev and M. A. Baribeau, "A New Algorithm for Digital Impedance Relays," *IEEE Trans. on Power App. Syst.*, Vol. 98, No. 6, pp.2232-2239, Dec. 1979.

[5] A. A. Girgis, "A New Kalman Filtering Based Digital Distance Relay," *IEEE Trans. on Power App. Syst.*, Vol. 101, No. 9, pp. 3471-3480, Sep. 1982.

[6] X.-N. Lin, M. Zhao, K. Alymann, P. Liu, "Novel Design of a Fast Phase Selector using Correlation Analysis," *IEEE Trans. on Power Del.*, Vol. 20, No. 2, pp. 1283-1290, Apr. 2005.

[7] S. A. Davari, S. M. Shahrtash, "Fault Classification in Distribution Power Lines Based on Electromagnetic Field Measurement and Fourier Transform," *IEEE PES Power Africa 2007 Conference and Exposition,* Johannesburg, South Africa, 16-20 July 2007.

[8] M. Kezunovic, I. Rikalo, D.J. Sobajic, "High Speed Fault Detection and Classification with Neural Nets," *Electric Power Systems Research Journal*, Vol. 34, No. 2, pp. 109-116, 1995.

[9] M. Kezunovic, I. Rikalo, D. Sobajic, "Real-Time and Off-Line Transmission Line Fault Classification Using Neural Networks, " *Intl. Journal of Engineering Intelligent Systems,* Vol. 4, No. 1, March 1996.

[10] S. Vasilic, M. Kezunovic, "Fuzzy ART Neural Network Algorithm for Classifying the Power System Faults," *IEEE Trans. on Power Del.*, Vol. 20, No. 2, pp. 1306-1314, Apr. 2005.

[11] A. Jamehbozorg, S. M. Shahrtash, "A Decision Tree-Based Method for Fault Classification in Single-Circuit Transmission Lines," *IEEE Trans. on Power Del.*, Vol. 25, No. 4, pp. 2190- 2196, Oct. 2010.

[12] A. Jamehbozorg, S. M. Shahrtash, "A Decision Tree-Based Method for Fault Classification in Double-Circuit Transmission Lines," *IEEE Trans. on Power Del.*, Vol. 25, No. 4, pp. 2184-2189, Oct. 2010.

[13] N. Zhang, M. Kezunovic, "Verifying the Protection System Operation Using an Advanced Fault Analysis Tool Combined with the Event Tree Analysis ", in Proc. of 36th Annual North American Power Symposium (NAPS), Moscow, Idaho, August, 2004

[14] M. Kezunovic, S. Vasilic, F. Gul-Bagriyanik, "Advanced Approaches for Detecting and Diagnosing Transients and Faults," Med Power 2002 Athens, Greece, Nov. 2002.

[15] B. Mahamedi, "A Novel Setting-Free Method for Fault Classification and Faulty Phase Selection by Using a Pilot Scheme," *2nd International Conference on Electric Power and Energy Conversion Systems (EPECS)*, 2011.

[16] M. Kezunovic, A. Esmaeilian, et. al. "Reliable Implementation of Robust Adaptive Topology Control," *HICCS - Hawaii International Conference on System Science, Manoa, Hawai*, January 2014.

[17] P. Dutta, A. Esmaeilian, M. Kezunovic, "Transmission-Line Fault Analysis Using Synchronized Sampling," *IEEE Trans. On Power Del.*, Vol. 29, No. 2, April 2014.

[18] A. Esmaeilian, "Evaluation and Performance Comparison of Power Swing Detection Algorithms in Presence of Series Compensation on Transmission Lines", *10th EEEIC*, pp. 89-93, 2011, Rome/Italy.

[19] M. Afzali, A. Esmaeilian, "A Novel Algorithm to Identify Power Swing Based on Superimposed Measurements", *11th EEEIC proceeding*, pp. 1109-1113, 18-25 May 2012, Venice/Italy.

[20] A. Esmaeilian, S. Astinfeshan, "A Novel Power Swing Detection Algorithm using Adaptive Neuro Fuzzy Technique," *International Conference on Electrical Engineering and Informatics (ICEEI2011)*, pp. 1-6, Bandung, 17-19 July, 2011.

[21] N. Zhang, M. Kezunovic, "A Study of Synchronized Sampling Based Fault Location Algorithm Performance under Power Swing and out-of-step Conditions," *Power Tech. 2005*, St. Petersburg, Russia, June 2005.

[22] A. Abdullah, A. Esmaeilian, G. Gurrala, P. Dutta, T. Popovic, M. Kezunovic, "Test Bed for Cascading Failure Scenarios Evaluation," *IPST 2013*, Vancouver, Canada, Jul 2013.

[23] A. Esmaeilian et. al., "A precise PMU based fault location method for multi terminal transmission line using voltage and current measurement," *10th EEEIC*, pp. 1-4, 2011, Rome/Italy.

[24] A. Esmaeilian, M. Kezunovic, "An impedance based fault location algorithm for tapped lines using local measurements," *NAPS 2013*.